Spectrochimica Acta Part A: Molecular and Biomolecular Spectroscopy 265 (2022) 120398

Contents lists available at ScienceDirect

Spectrochimica Acta Part A: Molecular and Biomolecular Spectroscopy

journal homepage: www.elsevier.com/locate/saa

First characterization of a Bronze Age textile fibre from Sardinia (Italy)

Roberta Iannaccone [a], Angela Antona [b], Donatella Magri [c], Alba Canu [d], Salvatore Marceddu [e], Antonio Brunetti [a,*]

[a] Università degli Studi di Sassari, Dipartimento di Chimica e Farmacia, Via Vienna 2, 07100 Sassari, Italy
[b] Independent Researcher, Former Scientific Director of Archaeological Excavation in La Prisgiona, Italy
[c] Università degli Studi di Roma "La Sapienza", Dipartimento di Biologia Ambientale, Piazzale Aldo Moro 5, 00185 Roma, Italy
[d] Conservatore Restauratore, Director of Centro di Restauro, Soprintendenza Archeologica, Belle Arti e Paesaggio per le Provincie di Sassari e Nuoro, Ministero per i Beni e le Attività Culturali, Italy
[e] Institute of Sciences of Food Production, National Research Council (ISPA-CNR), Sassari, Italy

HIGHLIGHTS

- The first discovery in Sardinia of yarn fibre belonging to the Bronze Age.
- Non-invasive and micro-invasive techniques applied to the study of Nuragic fibres.
- Archaeobotanical studies were applied to characterize the botanical species.
- Analytical techniques used to characterize cellulose content and its degradation.
- Micro-CT and SEM-EDS were applied to characterize the structure of the yarn.

GRAPHICAL ABSTRACT

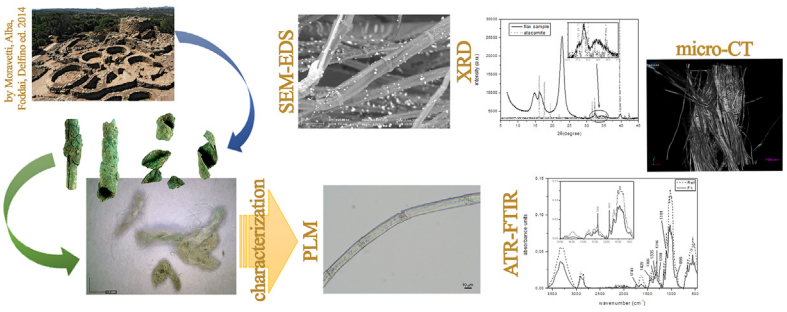

ARTICLE INFO

Article history:
Received 29 April 2021
Received in revised form 6 September 2021
Accepted 10 September 2021
Available online 16 September 2021

Keywords:
Bronze age yarn
Linen
PLM
ATR-FTIR
SEM-EDS
XRD
Micro-CT

ABSTRACT

This paper describes a case study of a linen yarn found inside a spiral bronze necklace fragment during an excavation campaign in la Prisgiona, a Nuragic settlement, near Arzachena, in north-east Sardinia. The site is one of the most interesting settlements of the Nuragic period. Abandoned after a fire, it was no longer inhabited, thus allowing the preservation of the Nuragic stratigraphy. The necklace fragments are part of a votive burial and the yarn is the only known textile material belonging to the Bronze Age period from Sardinia. The uniqueness of the finding, in the rare corpus of prehistoric textile materials, and the small amount of it available do not allow conventional analyses and requires a non-invasive/micro-invasive method. The protocol established to preserve as much as possible the entirety of the object, involving polarize light microscopy, portable ATR-FTIR, SEM-EDS, micro X-ray Computer Tomography and XRD, was successfully used to extend knowledge about the materials and techniques of this civilisation.

1. Introduction

La Prisgiona is an archaeological site mainly inhabited during the Bronze age (14th–8th century BCE) located near the modern city of Arzachena in north-east Sardinia (Italy).

* Corresponding author.
E-mail address: brunetti@uniss.it (A. Brunetti).

https://doi.org/10.1016/j.saa.2021.120398
1386-1425/

The site is an articulated Nuragic settlement located on the Punta d'Acu plateau, one of the most important complexes belonging to the river basin between the Liscia and San Giovanni rivers, an area rich in natural resources. The Nuragic civilisation emerged in the Early Bronze Age (approximately 18th century BCE) from cultures belonging to the Neolithic and the Copper Age, indigenous from Sardinia, that evolved in a more complex society after the discovery and use of metals (especially bronze). Besides the evolution of society and metallurgy arose the original architecture, identified by *Nuraghe* [1].

The archaeological site is composed of a central *Nuraghe* with a widespread village all around and no less than two giants' graves.

For its peculiar architecture, the *Nuraghe* plays a central role in the site. The tholos is protected by a first curved curtain wall with a wide courtyard and a well, whereas a second wall curtain corresponding to the bastion, incorporates also two side towers. The term *tholos* used also for Mycenaean graves, characterize the Nuragic structures belonging to the middle Bronze Age with a beehive-shaped chamber and a corbelled roof. The main difference with the Aegean structures is in the building above the ground of the *Nuraghe* [1].

The building was subsequently enlarged as a response to the evolving needs of the local population. A recent excavation attests that the site was occupied before a keep's fire and then abandoned for a long period until the Roman age (4th–5th century CE). The fire that occurred in the keep sealed the clayey floor where several artefacts were preserved, including fragments of ceramics [2–4].

Besides the daily instruments, some ceramics, stones and bronze objects were found placed in depressions inside the clayey stratum (Fig. 1).

One of these findings consisted of a potbelly amphora without the neck and part of the body and partially damaged by the fire. A miniature dagger, some spiral bronze fragments of a necklace and several plates were stored inside the amphora (Fig. 2) [5].

During the restoration, a small piece of suspended yarn was found inside one of the bronze fragments of the necklace.

This extraordinary finding is the only discovered fibre material in Sardinia belonging to this period.

Due to the perishable nature of the material, it is extremely difficult to find evidence of fibres in archaeological excavations. Rare evidence was found only in specific contexts with controlled environments favourable to preservation. For instance, most of the findings of linen textile fragments in Italy came from excavations near the Alpine lakes area or glaciers [6]. Most textiles were found preserved in association with metal artefacts or in any case mineralised [6].

Fig. 1. The floor of the keep with clayey stratum.

Fig. 2. Necklace fragments.

To a first examination, restorers assumed the use of a bast fibre, such as flax. Another hypothesis suggests the use of byssus, a fibre derived from a mollusc, renowned in Sardinia, whose findings date back to the Roman period [7,8]. We carried out different analyses to recognise the type of fibre, characterise its degradation and exclude the presence of hemp and wool, the use of which begins in the final Eneolithic – Early Bronze age and in the Middle-Late Bronze Age, respectively [6].

In order to preserve as much as possible the small amount of fibre, a completely non-invasive and micro-invasive approach has been used.

2. Materials and methods

Polarized light microscopy (PLM), portable Attenuated Total Reflectance Fourier Transform Infrared Spectroscopy (ATR-FTIR), Scanning Electron Microscope in Low Vacuum mode coupled with Energy Dispersive Spectrometer (SEM-EDS), micro X-ray Computer Tomography (micro-CT) and X-ray diffraction (XRD) were used in a non-invasive or micro-invasive way. The sample was small enough to be placed inside the XRD without additional manipulations and the mechanic characteristics of the material allowed to handle the pressure exerted by the portable ATR module of the FTIR spectrometer without evidence of damage. A small piece of yarn already detached from the bundle was used for micro-CT.

The piece was also used for the observation of the morphological features of the fibres through a polarised light microscope at high magnification, after separation of a single thread, and for SEM-EDS. These analyses were the only required micro-invasive procedures.

All plant fibres have a structure mainly composed of cellulose, hemicellulose, pectin, lignin and minor components such as waxes, inorganic materials, water and other impurities. The percentage of each component depends on the type of fibre and can vary also among different cultivation areas depending on factors such as latitude, precipitation, temperature and soil [9].

This variability affects the cellulose content and its composition impacting on the degradation conditions, which can vary also along the fibre length. For this reason, the sample was analysed in different areas to obtain average measures of the material.

ATR-FTIR analyses provided information mainly about cellulose, the more abundant substance in the sample. After the first recognition by portable optical microscopy, spectra acquired with ATR-FTIR were compared with a modern reference (beginning of

the 20th century) belonging to a linen fabric measured in the Clemente collection, stored in the archaeological and ethnographic Museum "G. Sanna" in Sassari (Italy).

The choice for the reference was driven by the opportunity to collect a reference as close as possible to the origin and manufacturing of our fibres. Modern yarns are all treated with chemicals and mechanical procedures, thus they are likely to provide mismatching with ancient samples, in addition, all the bast plant fibres have similar chemistry and microstructure. Some attempts at differentiation among bast fibres were published in literature but the results can be problematic when dealing with archaeological fibres [10,11].

The threads were analysed by portable ATR-FTIR to investigate the cellulosic content, its degradation and the presence of other organic and inorganic materials.

The spectra were acquired by a Bruker Alpha spectrometer with an operating range of 4000–375 cm^{-1}, a resolution of 4 cm^{-1}, SiC Globar source and DTGS detector equipped with ATR module with a monolithic diamond. The spectra were acquired in the absorbance mode. To obtain a good resolution 128 scans were performed for every spectrum. In addition, two measures were acquired for every point changing the orientation of the sample at 90°.

The spectra were elaborated with OPUS software by Bruker, with a concave rubber band correction for the background and 10 interactions.

Images of the fibres were taken with portable microscopes, Dino-Lite 1,3 Mpixel with polarised light, to document the state of preservation and the presence of small green crystals all over the surface.

Some fibres were separated from the bundle and analysed by a Zeiss Axiolab 5 optical microscope with polarized lenses. An external digital camera was used to acquire pictures.

XRD measure was performed using the D2 PHASER benchtop diffractometer (Bruker), with radiation CuKα_1 = 1.54 Å, operating at 30 kV, 10 mA, 2θ range 7°-50°, step size 0,02°, rotation speed of 2 rpm.

SEM-EDS was performed with a Zeiss EVO LS10, Environmental Scanning Electron Microscope, in low vacuum mode (LV), avoiding sample coating and mounted the sample on carbon stub. The analysis was performed with variable pressure (range 10–100 Pa) and the images were acquired using two detectors: a Variable pressure electron detector (VPSE) for secondary electrons (SE) and a Backscattered electron detector (BDS) for backscattered electrons (BSE). The elemental microanalysis was carried out with Energy Dispersive Spectrometer Inca X-Act (Oxford Instruments).

Micro-CT projection images were acquired with a Skyscan 1172 by Bruker, with a resolution of 1.1 μm, at 40 kV, 250 μA. The images were then transformed into a 3D model with NRECON software by Bruker. To obtain the projection images, the sample was placed on the rotating stub, with a minuscule quantity of wax on the base to maintaining the sample stood, practically without moving.

Three investigated areas were highlighted in this paper. Two measured points were acquired on a small thread, where both areas with and without green particles are visible (named respectively C1 and F1) and another point was compared on a loose thread (F2).

3. Results and discussion

Observations under the portable microscope show compact white threads with some green and dark yellow impurities stuck inside (Fig. 3).

Fig. 3. Detail of the sample acquired at 30×.

Only two areas of the bundle show an extended greenish aspect and a close observation reveals light green crystals trapped in the fibres.

Single fibres examined under the polarized light microscope, show typical dislocation (also called cross-thatches or nodes) and they were cylindrical in shape, with thick walls. Lumens were small and look like narrow lines. Small particles are visible all over the surface at high magnification (Fig. 4). Besides, the length (2 mm), width (16 μm) and morphology of the pointed end are consistent with the description of flax in the literature and its distinction from hemp [12–14].

Unfortunately, in both optical microscope observations and ATR-FTIR analysis, the sample could not be cleaned, due to its characteristics of uniqueness. The presence of particles on the fibre's surface slightly complicated the reading of the results, without completely affecting them.

Flax was one of the first domestic crops, originally cultivated for its oil-rich seeds and represents the earliest known domesticated fibre documented in the archaeological records [15,16]. Evidence of flax cultivated for being used as fibre textile was found in the southern Levant, during the Early Neolithic, and then slowly diffuse across Europe from the Middle to Late Neolithic [13,15].

The use of *Linum* fibres in Sardinia during the Bronze Age, reported here for the first time, is supported by the presence of *Linum usitatissimum* L. subsp. *angustifolium* (Huds.) Thell. a native plant in the island [17]. It is also supported by the archaeobotanical record of two seeds of *Linum* from the Chalcolithic site of Canelles (Selargius - Cagliari) [16], as well as by the finds of several seeds from the Bronze Age Nuragic site of Sa Osa (Cabras -Oristano) [18] and from the Iron Age nuraghe S'Urachi (San Vero Milis - Oristano) [19] witnessing its continuous usage through time.

Notably, the process of obtaining flax fibres remained almost unaltered until the beginning of the 20th century. It consists of four main steps: harvesting, removing and threshing capsules, retting stems and dressing the flax (breaking, scutching and heckling) [20]. All these practices are implemented to separate the wooden outer part with lignin from the fibres, mainly cellulose, used for textiles. Gleba, [21] and Gleba and Harris [22] suggest that the first bast fibres have not undergone the complete process but they are been only partially rettings.

Spectra of the sample in point F1 (Fig. 5) acquired in a white and almost completely clean area of the thread shows the band at 898 cm^{-1} characteristics of the amorphous region. The narrowing of the band reflects the low amount of disordered structure [23].

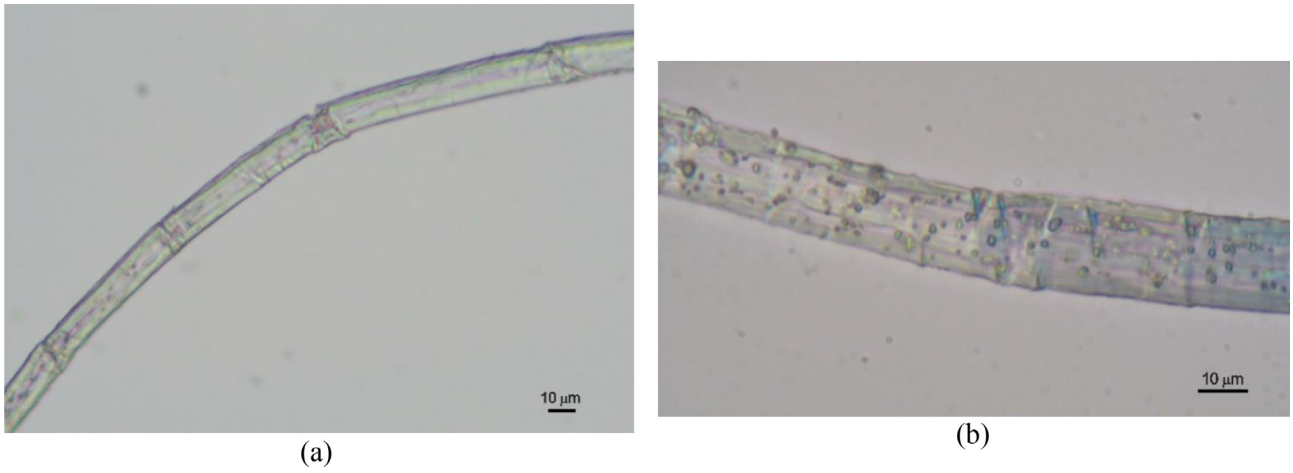

Fig. 4. Flax fibre with (a) polarized light, (b) differential interface contrast (DIC).

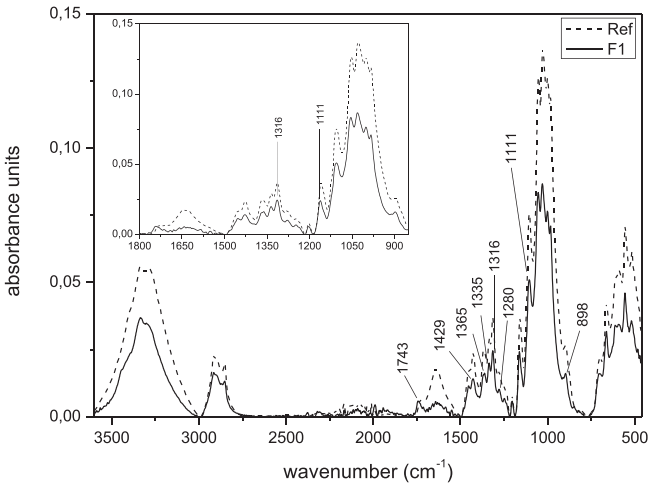

Fig. 5. Comparison between F1 spectrum, solid line, and reference, dotted line. In the magnification the region from 1800 cm^{-1} to 850 cm^{1}.

This band becomes more intense only in the spectrum of point C1 (Fig. 7).

The band at 1280 cm^{-1} relative to the CH_2 vibrations and characteristic of crystalline cellulose is weak in the spectrum but would not necessarily mean a low sample crystallinity (Fig. 5). A weak or absent band at 1280 cm^{-1} is reported in the literature for flax samples [23].

Cellulose undergoes changing caused by degradation processes occurring in the region from 1400 cm^{-1} to 1300 cm^{-1}. The three bands at 1365 cm^{-1}, 1335 cm^{-1} and 1316 cm^{-1}, correlated with CH and CH_2 vibrations, show a change in intensity compared with the reference, but not in the relative peak intensity (Fig. 5). In particular, bands at 1335 cm^{-1} and 1316 cm^{-1} demonstrate the presence of crystalline I cellulose. Bands at 1429 cm^{-1} and 1111 cm^{-1} can also be used as an indication for the presence of cellulose I, as mentioned in the literature [23].

In the spectra analysed, bands are slightly shifted (few units) to low wavenumber but not enough to consider those shifts as the presence of cellulose II or a sign of degradation processes [23]. More likely the shift is due to the technique used to acquire the spectra, together with the influences produced by dirt trapped into the bundle [24].

Literature [25] assigns the band at 1730 cm^{-1} to the carbonyl group that appears in some spectra analysed with ATR-FTIR. In point F2 and the reference sample, the band appears as a shoulder to the broader band of absorbed water, whereas some other measured points do not show the band at all (C1 and F1) or it is too low to be clearly distinguished by the water broad band. In the spectrum of point F1, appears a band at 1743 cm^{-1} that can be assigned to a degradation process of oxidation on the carbonyl group rather than to a shift caused by its surrounding, as it occurs in the bands mentioned before (Fig. 5). Oxidation functional groups such as aldehyde and keto absorb in this narrow region of the spectrum, between 1700 and 1750 cm^{-1} [24,26]. In addition, point F1 does not show any other shift of such entity in the spectrum (Fig. 5).

Both spectra F1 and F2 show a broad weak band at 1629 cm^{-1} corresponding to the vibration of water absorbed into cellulose chains, much lower in intensity compared with the reference sample (Fig. 5).

None of the analysed spectra shows the band at 1586 cm^{-1} indicative of lignin. The low content, characteristic of flax fibres, may have been further decreased during fibre processing [10].

In the green area, the observation on the portable microscope shows both small light green crystals and fibres with light green colouration (Fig. 6).

These green crystals may be attributed to the residues of copper alteration of the bronze necklace fragments.

Fig. 6. Thread end with few light green crystals acquired at 243×.

Comparison of ATR-FTIR spectra obtained from green areas shows two small absorptions at 3444 and 847 cm^{-1}, related to the copper corrosion products such as a basic copper chloride [27,28] (Fig. 7).

The intensity of both recognisable peaks is affected by the small quantity of the particles trapped in the fibres compared to the cellulosic material (Fig. 7).

The other bands visible in the spectrum of point C1 can be ascribed to the main cellulose content.

In each spectrum analysed, no further peaks were recognised useful to characterise the dark yellow material visible under the portable optical microscope.

Mineralised fibres can provide valuable information about the manufacturing of ancient textiles, thanks to the particular conditions of the burial environment. However, in this case, the fibres analysed cannot properly be ascribed as mineralised fibres, due to the absence of an actual "replacement of the physical shapes of fibres with minerals" as defined in the literature [29]. It can be defined rather as fibres with some minerals trapped in the bundle.

The well-preserved appearance of the yarn could be closely connected to the presence of copper-based crystals inside the bundle structure, as visible in the microscope images. The presence of copper acts as an inhibitor to microbial growth avoiding biodegradation and its mechanism is well described in the literature [30,31].

An attempt to calculate the crystallinity index was done using the ratio established by O'Connor et al. and Nelson and O'Connor, referred to as total crystallinity index (TCI), lateral order index (LOI) and Hydrogen-bond intensity (HBI) [32–34]. The ratio between 1430 cm^{-1} and 897 cm^{-1} is sensitive to the crystal structure, thus the LOI index is an evidence of the presence of cellulose I in the general cellulose structure. As expected, the reference has the highest LOI index, while the lowest is C1. The result of LOI for C1 is consistent with its highest intensity of amorphous band documented. Low values in LOI can also be seen as an indication for increasing access to the cellulose surface (Table 1). In this perspective, the presence of copper-based materials can affect the results [35].

TCI was calculated with the ratio between band at 1368 cm^{-1} and band at 2916 cm^{-1}. In any case, the TCI results cannot be compared and give inconsistent results due to the presence of two overlapping bands at 1368 and 1359 cm^{-1}. The HBI index represents both cellulose crystallinity and the amount of bounding water in the structure calculated as the ratio between 3335 cm^{-1} and 1336 cm^{-1} [34]. Table 1 shows the highest value for sample C1, not comparable with the results of LOI and TCI. This inconsistent result may be explained by the amount of OH bonding related to the presence of a copper-based mineral in the area, as atacamite - $Cu_2Cl(OH)_3$.

Table 1
Results of calculated LOI, TCI and HBI for every sample.

Sample	LOI	TCI	HBI
F1	0.88	1.00	1.85
C1	0.57	1.27	2.18
F2	0.68	1.36	2.00
Ref	0.92	1.14	1.97

However, other fibre components and impurities, although not visible in the spectra, can influence the final result of the bands' intensity. Besides, the method behind the ATR-FTIR technique and its susceptibility to slight changes in the band position significantly affects the crystallinity index calculation [34,36].

XRD analysis provides a comparative method to calculate the crystallinity index and to recognise different types of cellulose. Usually, fibres were pre-treated through grinding and then analysed to obtain a casual orientation of crystal structure. In the case presented the sample must be preserved as much as possible, thus it was analysed in one piece, providing a rotation of the plate during the analysis to overcome this problem.

The crystallinity index was calculated through the Segal method [37]:

$$CI = \frac{I_{200} - I_a}{I_{200}}$$

where I_{200} is the total intensity at 22.8° 2θ assigned to crystalline cellulose fraction, and I_a is the intensity of the amorphous cellulose fraction at 18° 2θ. The spectrum was corrected for background and intensities for crystallographic planes and the amorphous phase were calculated, confirming the well-preserved structure with a CI of 78,8%.

The result is consistent with those emerging from the ATR-FTIR even if the use of this formula face some risks of overestimating the value of CI [38].

The diffractogram also shows the two reflections at 14,91° 2θ and 16,39° 2θ respectively assigned to (1 –1 0) and (1 1 0) crystallographic planes. Moreover, analysis shows the absence of cellulose II, the degraded crystalline phase of cellulose I (Fig. 8).

In addition to peaks related to cellulose, two small peaks are visible at 32,35° 2θ and 39,73° 2 θand appear in correspondence

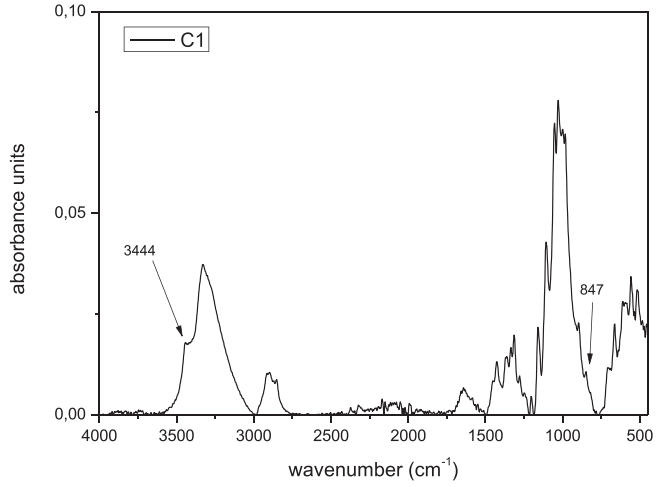

Fig. 7. Spectrum C1 with the indication of bands attributed to a basic copper chloride.

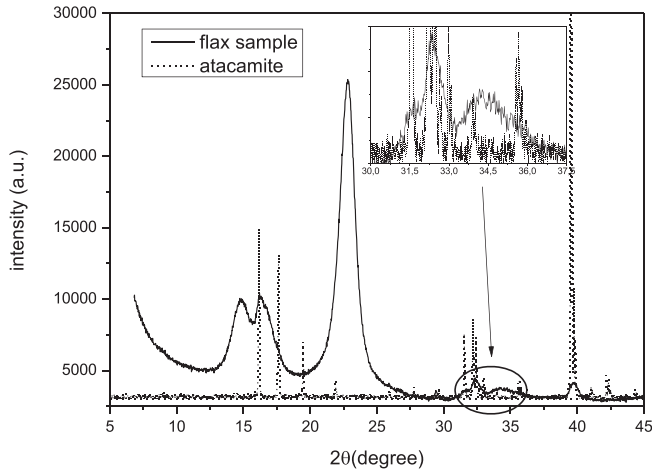

Fig. 8. Comparison between sample spectrum, solid line, and atacamite reference spectrum, dotted line. In the magnification the region from 30° to 37,5°.

of the (210) and (200) crystallographic planes of basic copper chloride, atacamite [39,40]. Cellulose I usually shows a broad peak at 34,5° 2θcomposite of several reflections where the crystallographic plane (004) is also visible but not predominant [41]. Spectrum show this peak closed to the peak at 32,35° 2θbut they do not interfere with each other (Fig. 8).

The peaks attributed to atacamite are weak and broad due to the small quantity of material, but the diffractogram excludes the presence of copper carbonate, even if traces of calcium were found in other analyses. Comparison with the ATR-FTIR spectrum of the green area (C1) can confirm the hypothesis of the presence of atacamite.

To confirm the assumptions made on the type of bast fibre, crystallinity and residues of copper degradation, SEM-EDS was performed.

SEM images show the presence of widespread microparticles of copper all around the fibres, which have preserved them from biological attacks (Fig. 9). This presence of copper all over the sample can explain the absence of a high level of degradation, usually visible in such ancient fibres, and consequently their high crystallinity values obtained with ATR-FTIR and XRD.

EDS microanalyses on areas with copper particles highlight the presence, besides the copper, of chlorine and traces of calcium. The acquisition of an elemental map of these elements on an isolated fibre allows recognising that copper and chlorine are visible in the same area of the spots visible on the BSE image, confirming the presence of atacamite as degradation products of the bronze necklace beads (Fig. 10).

Calcium, on the other side, does not follow the fibre edges and it is visible more or less in the whole image, excluding the presence of cristals of calcium oxalate (Fig. 10).

The absence of cristals of calcium oxalate can support the fibre's attribution to flax [42].

In addition to an extended presence of small particles of atacamite, the high crystallinity resulted in such an old sample can be due to the deterioration of the cementing materials, mostly amorphous, which increases the packing of cellulose chains [43,44].

The hypothesis is that besides the biocide action of copper, which preserves cellulosic material from biological attacks, high CI could also be related to the more intense degradation process in the amorphous cellulose components together with the highest crystalline nature of the flax [9].

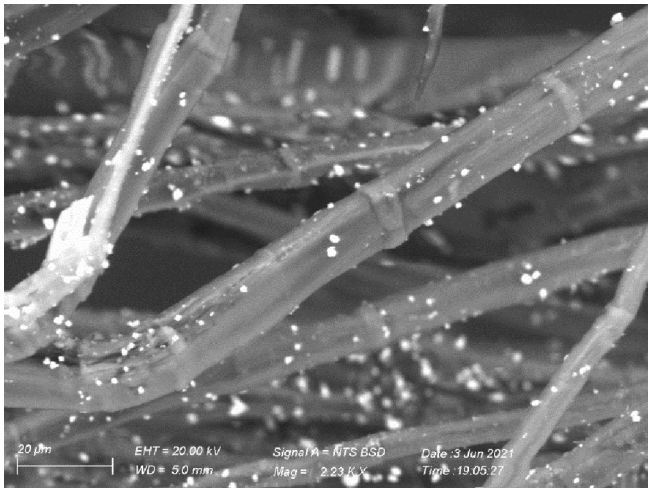

Fig. 9. BSE image at 2230× of the fibre and atacamite particles.

Regarding the yarn and its spinning, the observation to portable microscope showed the plying of two threads in the S-direction, with a minimal twisting of the single thread (Fig. 11) [21].

3D reconstruction to micro-CT, can provide a more straightforward image of the single threads twisting [45]. The same detached piece used for micro-invasive techniques was previously used to performs micro-CT and provide a better and more detailed 3D model of the threads.

Images confirm the S-direction for the ply of the yarn, and it is also possible to observe the s-direction of the twisting for both single threads (Fig. 12). This S2s configuration of the yarn was attested for several linen textiles belonging to the Chalcolithic period from the southern Levant [46–48].

A possible hint about its spinning is provided by SEM images show in many areas of the thread the dislocations of fibres adjacent to each other. The observation of these detail can suggest splicing as the spinning technique to obtain the yarn [22], even if optical microscopy and SEM images do not show the presence of residual epidermal tissue, nor FTIR spectra show the presence of pectin or gum, derivated by a partial retting and suggested as a possible binding material to keep together the fibres during the splicing.

Cooke, El-Gamal, & Brennan, [49] suggest the use of a water-based adhesive to maintaining the fibres together during the splicing, such as saliva. In Sardinia, also in the modern time, women used to chew roasted broad beans to increase salivation and kept the flax fibres wet while spinning [50], thus this technique with saliva might be already used in the past to spliced the fibres.

Nevertheless, binding materials could have disappeared during the burial as mentioned before or for several treatments [22].

Some examples of spliced plant fibre threads used to connect small bronze objects (appliques and buttons) were found in the Tomba del Guerriero (Tarquinia) and Villanova fossa burial (Vulci) [21]. These examples belong to a later period (7th and 8th century BCE) but could be closely related to the technique used for the sample analysed, although, the sample was too small and fragmented to ensure proper identification of the spinning technique.

4. Conclusions

The analyses were conducted on a finding of a well-preserved flax bundle belonging to the Nuragic site of La Prisgiona. The sample is the only findings of organic material related to this civilization. Due to its nature, this unique piece of textile material dated to the Bronze Age has been analysed with a non-invasive and micro-invasive protocol, allowing us to investigate the sample without destroying it.

The threads were recognised as flax (*Linum usitatissimum* L.) by observation of fibres under the polarised optical microscope, and SEM-EDS, from their morphological characteristics. This statement is supported by the autochthony of *Linum usitatissimum* subsp. *angustifolium* (Huds.) Thell. and by various finds of *Linum* seeds in Chalcolithic to Iron Age sites in Sardinia. Unfortunately, the analysis under the polarized microscope cannot provide further information to recognise fibrillar orientation.

ATR-FTIR and XRD provided further information about crystallinity, ageing and its preservation.

SEM confirms also the presence of crystals of atacamite, already detected with ATR-FITR and XRD, with the aid of elemental maps and excludes the presence of calcium oxalate crystals, supporting the recognition of bast fibre as flax.

Results show a well-preserved bundle of fibres that can be associated with multiple factors. The absence of light, a common cause of oxidation and intermolecular bond-breaking, with the peculiar preservation site within a bronze bead and the presence of small crystals of atacamite on the fibres surface, known for its biocide

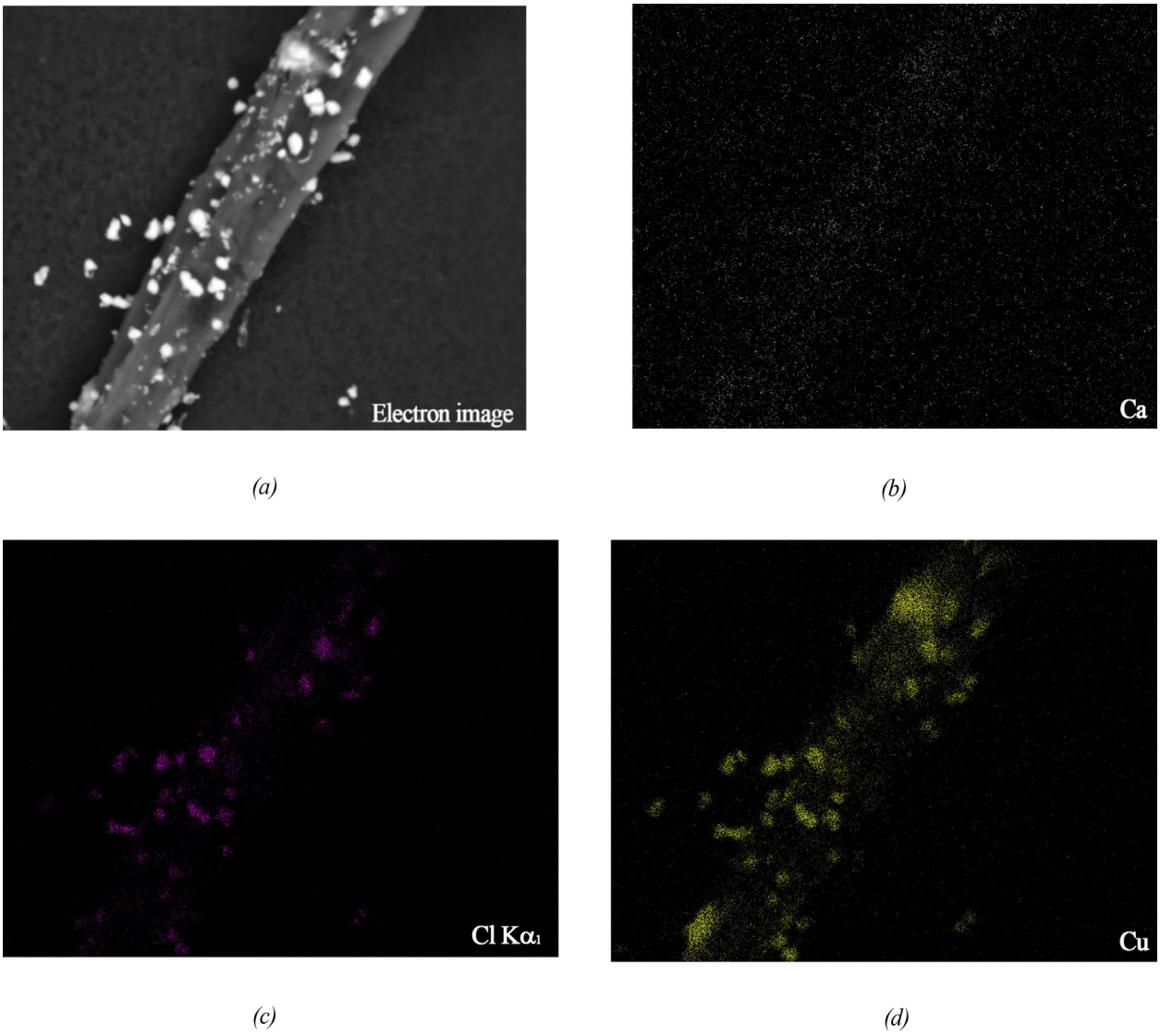

Fig. 10. Image of investigated area (a) and the elemental map of calcium (b), chlorine (c) and copper (d).

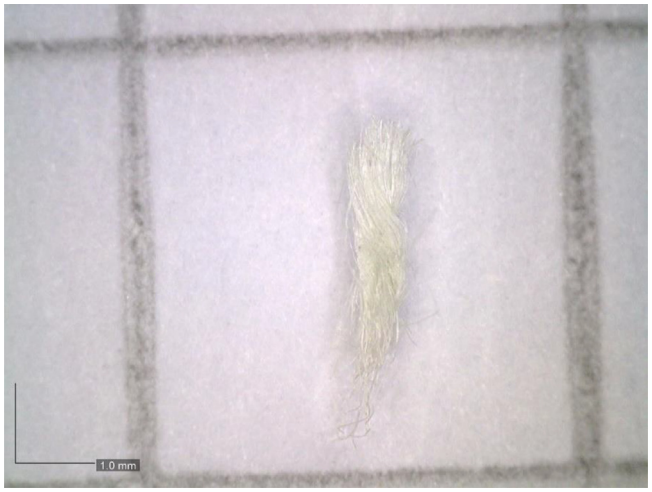

Fig. 11. Detail of a fibre's fragment plying with S-direction.

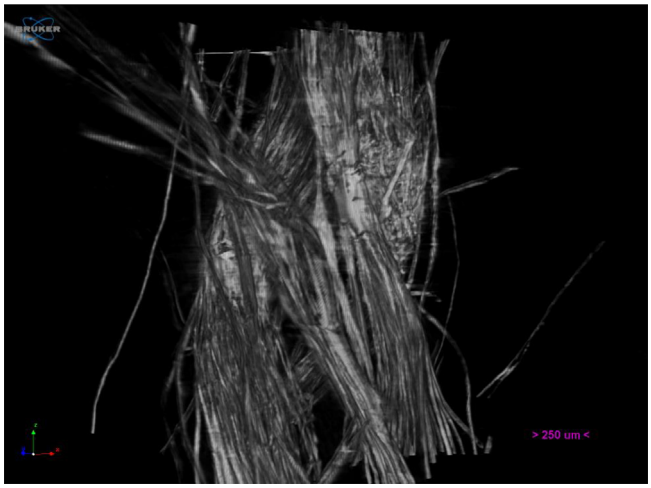

Fig. 12. Micro-CT of the fragment.

characteristic, may have prevented the degradation of cellulosic chains.

Besides these two factors, the hypothesis supported by the analyses is a preferential way of the degradation of amorphous contents earlier than the crystalline chains of cellulose.

Only one point shows a weak band related to the oxidation of the carbonyl group, while in general, the LOI index value related to the highest crystallinity form of cellulose (cellulose I) in points analysed appears consistent with the literature.

XRD also provides a high value of crystallinity index confirming and supporting what emerges from ATR-FTIR analysis.

The analysis of the spinning method suggests the spliced techniques with two threads plying with S-direction, but the amount of fibre can not completely provide proper identification.

The non-invasive and micro-invasive protocol used, achieve successful results for the characterization of the artefact while preserving its integrity.

CRediT authorship contribution statement

Roberta Iannaccone: Investigation, Writing original draft, Writing review and editing, Resources. **Angela Antona:** Investigation. **Donatella Magri:** Investigation. **Alba Canu:** Investigation. **Salvatore Marceddu:** Investigation. **Antonio Brunetti:** Investigation, Supervision, Writing original draft, Resources, Funding acquisition

Declaration of Competing Interest

The authors declare that they have no known competing financial interests or personal relationships that could have appeared to influence the work reported in this paper.

Acknowledgements

This work was supported by Programma Operativo Nazionale (PON) Ricerca e Innovazione 2014–2020 – Asse I "Capitale umano", Azione I.2 A.I.M. "Attrazione e Mobilità Internazionale dei Ricercatori", D.D. del MIUR n. 407 del 27 febbraio 2018 - Linea 2 "Mobilità" [AIM1843180-3 – CUP J54I18000380001] (Roberta Iannaccone) and FAR 2019, FAR 2020 and FSC 2014-2020 project by Regione Autonoma della Sardegna, "Sviluppo di una metodologia spettroscopica integrata e innovativa per la caratterizzazione di bronzi antichi" (RASSR79938,CUP J81G17000140002) (Antonio Brunetti).

The authors want to thank Prof. Marco Curini Galletti for providing support in the acquisition of images by the optical microscope, Dr. Emma Cantisani, ISPC -CNR Florence for her useful support in the XRD technique, Franca Liliana Casiddu for her work of restoration on necklace fragments and Salvatore Sechi for the documentation photos of the archaeolo.

gical artefacts, Centro di Restauro, Soprintendenza Archeologica, Belle Arti e Paesaggio per le Provincie di Sassari e Nuoro, MIBAC.

The authors are grateful to CIRTEBEC - Centro Interuniversitario di Ricerca sulle Tecnologie per i Beni Culturali-*GAUSS* Laboratories of the Università degli Studi di Sassari with the support of Regione Autonoma della Sardegna, for providing instrumentation and Prof. Giacomo Oggiano, University of Sassari, for SEM-EDS.

References

[1] P. Melis, The nuragic civilization, Carlo Delfino editore, 2003.
[2] A. Antona, Arzachena, Pietre senza tempo, Carlo Delfino editore, 2013.
[3] A. Antona, Nota preliminare sui contesti stratigrafici della Gallura nuragica: l'esempio di La Prisgiona di Arzachena, in: Atti della XLIV Riunione Scientifica dell'Istituto Italiano di Preistoria e Protostoria 23–28 novembre 2009, II, 2012, pp. 687–696.
[4] M. Milletti, Cimeli d'identità: tra Etruria e Sardegna nella prima età del ferro, Officina edizioni, 2012.
[5] A. Antona, S. Puggioni, Spazi domestici, società e attività produttive nella Sardegna nuragica. L'esempio della Gallura, in: L'espai domèstic i l'organització de la societat a la protohistòria de la Mediterrànea occidental (Ier mil-lenni a. C.)", Actes de la IV Reunió Internacional d'Arqueologia de Calafell (Calafell – Tarragona, 6 al 9 de març de 2007), Arqueo Mediterrànea 11/2, 2009, pp. 331–348.
[6] M. Gleba, Italian Textiles from Prehistory to Late Time, in: A Stitch in Time: Essays in Honour of Lise Bender Jørgensen, Gothenburg University, 2014, pp. 145–169.
[7] F. Maeder, Sea-silk in aquincum: first production proof in antiquity, Purpureae Vestes II. Text. Dye. Antiq., 2008, pp. 109–118.
[8] F. Maeder, Sea-silk–The rediscovery of the ancient textile material raises new questions, 2018, [Online]. Available: http://costume.mini.icom.museum/wp-content/uploads/sites/10/2018/12/Felicitas_Maeder_Toronto_article_PDF.pdf.
[9] L. Yan, N. Chouw, K. Jayaraman, Flax fibre and its composites - A review, Compos. Part B Eng. 56 (2014) 296–317, https://doi.org/10.1016/j.compositesb.2013.08.014.
[10] P. Garside, P. Wyeth, Identification of Cellulosic Fibres by FTIR Spectroscopy I: Thread and Single Fibre Analysis by Attenuated Total Reflectance, Stud. Conserv. 48 (4) (2003).
[11] P. Garside, P. Wyeth, Identification of cellulosic fibres by FTIR spectroscopy: Differentiation of flax and hemp by polarized ATR FTIR, Stud. Conserv. 51 (3) (2006) 205–211, https://doi.org/10.1179/sic.2006.51.3.205.
[12] M.-L.-E. Florian, D.P. Kronkright, R.E. Norton, The conservation of artifacts made from plant materials, Getty Conservation Institute, Los Angeles, 1990.
[13] R. Gale, D.F. Cutler, Plants in archaeology: identification manual of vegetative plant materials used in Europe and the Southern Mediterranean to c. 1500, 2000.
[14] I. Markova, Textile Fiber Microscopy, John Wiley & Sons Ltd, 2019.
[15] S. Harris, Flax fibre : Innovation and Change in the Early Neolithic A Technological and Material Perspective, Text. Soc. Am. Symp. Proc., 2014, pp. 1–10, [Online]. Available: http://digitalcommons.unl.edu/tsaconf/913.
[16] I. Camarda, C. Loi, Flax processing in Sardinia : a millenary material and non-material practice, 2012.
[17] F. Bartolucci et al., An updated checklist of the vascular flora native to Italy, Plant Biosyst. - An Int. J. Deal. Asp Plant Biol. 152 (2) (2018) 179–303, https://doi.org/10.1080/11263504.2017.1419996.
[18] D. Sabato et al., Archaeobotanical analysis of a Bronze Age well from Sardinia: A wealth of knowledge, Plant Biosyst. - An Int. J. Deal. Asp Plant Biol. 149 (1) (2015) 205–215, https://doi.org/10.1080/11263504.2014.998313.
[19] G. Pérez-Jordà, J. Hurley, D. Ramis, P. van Dommelen, Iron Age botanical remains from nuraghe S'Urachi Sardinia, Antiquity 94 (374) (2020), https://doi.org/10.15184/aqy.2020.33.
[20] U. Maier, H. Schlichtherle, Flax cultivation and textile production in Neolithic wetland settlements on Lake Constance and in Upper Swabia (south-west Germany), Veg. Hist. Archaeobot. 20 (6) (2011) 567–578, https://doi.org/10.1007/s00334-011-0300-8.
[21] M. Gleba, Textiles in pre-Roman Italy: from qualitative to quantitative approach, Orig. Preist. e protostoria delle civiltà antiche (40) (2018) 1, https://doi.org/10.17863/CAM.20482.
[22] M. Gleba, S. Harris, The first plant bast fibre technology: identifying splicing in archaeological textiles, Archaeol. Anthropol. Sci. 11 (5) (May 2019) 2329–2346, https://doi.org/10.1007/s12520-018-0677-8.
[23] K. Kavkler, N. Gunde-Cimerman, P. Zalar, A. Demšar, FTIR spectroscopy of biodegraded historical textiles, Polym. Degrad. Stab. 96 (4) (2011) 574–580, https://doi.org/10.1016/j.polymdegradstab.2010.12.016.
[24] C. Margariti, The application of FTIR microspectroscopy in a non-invasive and non-destructive way to the study and conservation of mineralised excavated textiles, Herit. Sci. 7 (1) (2019) 1–14, https://doi.org/10.1186/s40494-019-0304-8.
[25] M.R. Derrik, D. Stulik, J.M. Landy, Infrared Spectroscopy in Conservation Science, The Getty Conservation Institute, Los Angeles, 1983.
[26] S. Coseri et al., One-shot carboxylation of microcrystalline cellulose in the presence of nitroxyl radicals and sodium periodate, RSC Adv. 5 (104) (2015) 85889–85897, https://doi.org/10.1039/c5ra16183e.
[27] N.H. Tennent, K.M. Antonio, Bronze disease: synthesis and characterisation of botallackite, paratacamite and atacamite by infra-red spectroscopy, in: ICOM Committee for Conservation 6th triennial meeting: Ottawa, 21–25 September 1981: preprints, 1981, pp. 11.
[28] W. Martens, R.L. Frost, P.A. Williams, Raman and infrared spectroscopic study of the basic copper chloride minerals - Implications for the study of the copper and brass corrosion and "bronze disease", Neues Jahrb. fur Mineral. Abhandlungen 178 (2) (2002) 197–215, https://doi.org/10.1127/0077-7757/2003/0178-0197.
[29] H.L. Chen, K.A. Jakes, D.W. Foreman, Preservation of archaeological textiles through fibre mineralization, J. Archaeol. Sci. 25 (10) (1998) 1015–1021, https://doi.org/10.1006/jasc.1997.0286.
[30] P. Tiano, Biodegradation of Cultural Heritage: Decay Mechanisms and Control Methods, CNR-Centro di Stud. Sulle Cause Deperimento e Metod. Conserv. Opere d'Arte, vol. 9, 2001, pp. 1–37, [Online]. Available: http://www.arcchip.cz/w09/w09_tiano.pdf.
[31] H.L. Chen, K.A. Jakes, D.W. Foreman, SEM, EDS, and FTIR Examination of Archaeological Mineralized Plant Fibers, Text. Res. J. 66 (4) (1996) 219–224, https://doi.org/10.1177/004051759606600406.

[32] R.T. O'Connor, E.F. DuPrè, M. D, Application of infrared absorption spectroscopy to investigation of cotton and modified cottos: Part I: physical and crystalline modification and oxidation, Text. Res. J. 28 (5) (1958) 382–392.
[33] M.L. Nelson, R.T. O'Connor, Relation of certain infrared bands to cellulose crystalinity and crystal latticed type. Part II. A new infrared ratio for estiamation of crystallinity in cellulose I and II, J. Appl. Polym. Sci. 8 (3) (1964) 1325–1341.
[34] J. Široký, R.S. Blackburn, T. Bechtold, J. Taylor, P. White, Attenuated total reflectance Fourier-transform Infrared spectroscopy analysis of crystallinity changes in lyocell following continuous treatment with sodium hydroxide, Cellulose 17 (1) (2010) 103–115, https://doi.org/10.1007/s10570-009-9378-x.
[35] I. Spiridon, C.A. Teacă, R. Bodîrlău, Structural changes evidenced by ftir spectroscopy in cellulosic materials after pre-treatment with ionic liquid and enzymatic hydrolysis, BioResources 6 (1) (2011) 400–413, https://doi.org/10.15376/biores.6.1.400-413.
[36] M. Poletto, H.L. Ornaghi Júnior, A.J. Zattera, Native cellulose: Structure, characterization and thermal properties, Materials (Basel) 7 (9) (2014) 6105–6119, https://doi.org/10.3390/ma7096105.
[37] L. Segal, J.J. Creely, A.E. Martin, C.M. Conrad, An Empirical Method for Estimating the Degree of Crystallinity of Native Cellulose Using the X-Ray Diffractometer, Text. Res. J. 29 (10) (1959) 786–794, https://doi.org/10.1177/004051755902901003.
[38] A.D. French, M. Santiago Cintrón, Cellulose polymorphy, crystallite size, and the Segal Crystallinity Index, Cellulose 20 (1) (2013) 583–588, https://doi.org/10.1007/s10570-012-9833-y.
[39] D.A. Scott, A review of copper chlorides and related salts in bronze corrosion and as painting pigments, Stud. Conserv. 45 (1) (2000) 39–53, https://doi.org/10.1179/sic.2000.45.1.39.
[40] B. Lafuente, R.T. Downs, H. Yang, N. Stone, The power of databases: The RRUFF project, in: T. Armbruster, R.M. Danisi (Eds.), Highlights in Mineralogical Crystallography, W. De Gruyter, Berlin, 2015, pp. 1–30.
[41] A.D. French, Idealized powder diffraction patterns for cellulose polymorphs, Cellulose 21 (2) (2014) 885–896, https://doi.org/10.1007/s10570-013-0030-4.
[42] C. Bergfjord, B. Holst, A procedure for identifying textile bast fibres using microscopy: Flax, nettle/ramie, hemp and jute, Ultramicroscopy 110 (9) (Aug. 2010) 1192–1197, https://doi.org/10.1016/j.ultramic.2010.04.014.
[43] Y. Cao, F. Chan, Y.H. Chui, H. Xiao, Characterization of flax fibres modified by alkaline, enzyme, and steam-heat treatments, BioResources 7 (3) (2012) 4109–4121, https://doi.org/10.15376/biores.7.3.4109-4121.
[44] D. Tamburini et al., The short-term degradation of cellulosic pulp in lake water and peat soil: A multi-analytical study from the micro to the molecular level, Int. Biodeterior. Biodegrad. 116 (2017) 243–259, https://doi.org/10.1016/j.ibiod.2016.10.055.
[45] N. Haleem, X. Liu, C. Hurren, S. Gordon, S.S. Najar, X. Wang, Investigating the cotton ring spun yarn structure using micro computerized tomography and digital image processing techniques, Text. Res. J. 89 (15) (Aug. 2019) 3007–3023, https://doi.org/10.1177/0040517518805387.
[46] Y. Goldman, R. Linn, O. Shamir, M. Weinstein-Evron, Micro-RTI as a novel technology for the investigation and documentation of archaeological textiles, J. Archaeol. Sci. Reports 19 (Jun. 2018) 1–10, https://doi.org/10.1016/j.jasrep.2018.02.013.
[47] J. Levy, I. Gilead, Spinning in the 5th millennium in the Southern Levant: Aspects of the Textile Economy, Paléorient 38 (1) (2012) 127–139, https://doi.org/10.3406/paleo.2012.5463.
[48] O. Shamir, Textiles, Basketry and Cordage from Cave Q27, Contract Archaeol. Reports V (2015) 77–90.
[49] W.D. Cooke, M. El-Gamal, A. Brennan, The hand-spinning of ultra-fine yarns, part 2, Spinn. flax. CIETA Bull. 69 (1991) 17–23.
[50] P. Piquereddu, Tessuti. Tradizione e innovazione della tessitura in Sardegna, Ilisso Edizioni, Collana di. Nuoro, 2006.